JOURNAL OF BACTERIOLOGY, Apr. 1994, p. 2172–2176
0021-9193/94/$04.00+0

Vol. 176, No. 8

Pyruvate Metabolism in *Halobacterium salinarium* Studied by Intracellular ^{13}C Nuclear Magnetic Resonance Spectroscopy

SUKESH R. BHAUMIK AND HARIPALSINGH M. SONAWAT*

Chemical Physics Group, Tata Institute of Fundamental Research, Bombay-400 005, India

Received 18 October 1993/Accepted 7 February 1994

^{13}C nuclear magnetic resonance spectroscopy was used to study the metabolism of [2-^{13}C]pyruvate in intact cells of *Halobacterium salinarium*. The spectra of these cells show that pyruvate is reduced to lactic acid and transaminated to alanine. The intensity of C-2 lactate is higher under anaerobic conditions than under aerobic conditions. When cells are grown in the absence of glucose, the level of C-2 lactate intensity is lower. In extracts of these cells, the level of NADH-dependent lactate dehydrogenase activity is lower than that of cells grown in the presence of glucose. A C-5 glutamate resonance suggests the entry of pyruvate into the tricarboxylic acid cycle through acetyl-coenzyme A. In addition, the label is also observed at C-3 and C-4 of glutamate, signifying a pyruvate carboxylase-type reaction and scrambling of label at the fumarate-succinate stage plus malic enzyme operation, respectively. Citrate synthase and malic enzyme activity appear to be controlled by the growth conditions of *H. salinarium*.

Extremely halophilic bacteria are chemoorganotropic organisms whose growth requires the presence of unusually high concentrations of sodium and magnesium ions. Despite their reputation as organisms with limited metabolic activity who make a living by using amino acids (16), a number of diverse extreme halophiles metabolize carbohydrates and are reported to have several enzyme activities associated with carbohydrate utilization (7). Metabolism of trioses in *Halobacterium salinarium*, in contrast, has received scant attention specifically in relation to the tricarboxylic acid cycle and other anaplerotic routes feeding into the tricarboxylic acid cycle and the efflux of carbon units from the tricarboxylic acid cycle. Two succinate dehydrogenases with different apparent K_ms for succinate (10), an α-ketoglutarate dehydrogenase (13), glutamate dehydrogenase (5), and pyruvate:ferredoxin oxidoreductase (21) have been reported in *H. salinarium*. Although the enzymes of glyoxylate and tricarboxylic acid cycles have been detected in *H. salinarium* (1), the information is far from complete. One of the major reasons for this has been the lack of information about the stability of the enzymes in vitro.

^{13}C nuclear magnetic resonance (NMR) spectroscopy, starting with enriched substrates, has been used to measure specific labelling at each site in metabolic intermediates (2, 4, 8, 9, 19, 20). Recently, mathematical modelling of the tricarboxylic acid cycle from labelling of glutamate C-1 to C-5 and the ^{13}C spin-spin coupling pattern observed because of enriched adjacent carbons in this amino acid has been reported (12, 18).

We have used ^{13}C NMR spectroscopy to study the tricarboxylic acid cycle and other related pathways in intact cells of *H. salinarium*. This strategy, in addition to offering the usual advantages of intracellular NMR spectroscopy, in our case, makes redundant uncertainty about the enzymes' stability in an in vitro milieu in studies of metabolic pathways. The results of our experiments are presented in this paper.

MATERIALS AND METHODS

[2-^{13}C]pyruvate was obtained from Isotec, and peptone (L-37) was obtained from Oxoid. [1-^{13}C]acetate, $NADP^+$, and NADH were obtained from Sigma. Other chemicals were reagent grade and were used as supplied.

H. salinarium (M1) culture (kindly provided by A. K. Singh, Department of Chemistry, Indian Institute of Technology, Bombay) was maintained and propagated in a medium consisting of 250 g of NaCl, 2 g of KCl, 20 g of $MgSO_4 \cdot 7H_2O$, and 10 g of peptone per liter (23). This was supplemented with 1% glucose or acetate where required. Cells were grown in a rotary shaker at 37°C and 150 rpm. Five percent of the 70-h culture was used for further propagation. Cells were harvested after 70 h by centrifugation at 1,200 × *g* for 30 min and were suspended (20% [wt/vol]) in basal salt medium (growth medium without peptone) prepared in D_2O. For cell extract preparation, the cells were suspended in 0.1 M Tris-HCl buffer (pH 7.2) containing 1.2 M NaCl, sonicated at 60 W for 2 min (eight times for 15 s each) with a Branson B30 Sonifier, and centrifuged at 33,000 × *g* for 30 min. The clear supernatant was used as cell extract.

^{13}C NMR experiments were performed with a ^1H-^{13}C dual probe at 125.76 MHz on a Bruker AMX500 spectrometer. The spectra were recorded with a 90° flip angle, with a 29,411.77-Hz spectral width and 16,384 datum points corresponding to a 0.28-s acquisition time and a digital resolution of 16 Hz per point. Powergated heteronuclear broadband decoupling of protons was used to minimize dielectric heating. A 39-dB power was used during relaxation delay (3 s), and 22 dB was used for decoupling during acquisition. A total of 512 transients were accumulated for each spectrum. Exponential multiplication leading to an additional line broadening of 10 Hz was applied prior to Fourier transformation of the free induction decays. Experiments were started by adding solid [2-^{13}C]pyruvate to 0.5 ml of cell suspension in a 5-mm NMR tube maintained at 27°C. Resonance assignments were done by recording authentic metabolites in basal salt medium and using corresponding peak positions. Chemical shifts are expressed in parts per million with respect to sodium 3-trimethylsilyl propionate, which was used as an external reference.

Malic enzyme was assayed spectrophotometrically by monitoring the reduction of $NADP^+$ at 340 nm. The reaction mixture consisted of 1.5 mM malate, 0.4 mM $NADP^+$, 6.0 mM $MnCl_2$, and cell extract in a final volume of 2.0 ml in 0.1 M Tris-HCl buffer (pH 9.0) containing 4.0 M NaCl.

* Corresponding author. Phone: 91222152971, ext. 2271. Fax: 91222152110. Electronic mail address: HMS@TIFRVAX.BITNET.

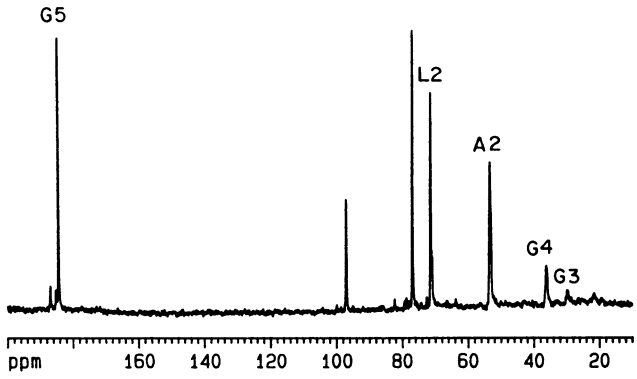

FIG. 1. Proton-decoupled ^{13}C NMR spectrum of *H. salinarium* cells grown in the presence of glucose after incubation with [2-^{13}C]pyruvate. The peak assignments are as follows: A2, C-2 of alanine; G3 to G5, C3 to C5 of glutamate, respectively; L2, C-2 of lactate.

Lactate dehydrogenase was assayed spectrophotometrically by monitoring the oxidation of NADH at 340 nm. The reaction mixture consisted of 1.0 mM pyruvate, 0.2 mM NADH, and cell extract in a final volume of 2 ml in 0.1 M Tris-HCl buffer (pH 7.5) containing 4.0 M NaCl.

A unit of enzyme activity was defined as the amount which reduces 1 μmol of $NADP^+$ (in the case of malic enzyme) or oxidizes 1 μmol of NADH (in the case of lactate dehydrogenase) per min under the conditions mentioned above. The level of protein was estimated by the method of Lowry et al. (17), with bovine serum albumin as a standard.

RESULTS AND DISCUSSION

To study the metabolism of pyruvate, ^{13}C NMR spectra of *H. salinarium* cells grown in various media (with or without glucose or the presence of acetate) and incubated under different conditions were recorded.

Formation of lactate and alanine. Spectra obtained from cells grown in media containing glucose and incubated with [2-^{13}C]pyruvate are presented in Fig. 1. Resonances at 53.5 and 71.3 ppm are assigned to C-2 of alanine and C-2 of lactate, respectively. Under anaerobic incubation (nitrogen bubbled through the cell suspension [Fig. 2b]), the intensity of the 71.3-ppm signal is greater than when the incubation is aerobic (oxygen bubbled through the suspension [Fig. 2a]). This is as expected from the lactate dehydrogenase reaction, which is much more pronounced anaerobically. Under these conditions, utilization of pyruvate through the tricarboxylic acid cycle is reduced and a relatively larger amount is available for the lactate dehydrogenase reaction.

Figure 3 shows the ^{13}C spectrum obtained from *H. salinarium* cells grown in the absence of glucose and incubated with [2-^{13}C]pyruvate. The intensity of lactate resonance is decreased compared with that in the presence of glucose (Fig. 1). Measurements of enzyme activity in extracts of these cells indicated that the level of pyruvate-dependent oxidation of NADH is 25% lower in these cells than that in cells grown in the presence of glucose. Spectra from cells grown in the presence of acetate (Fig. 4) and activity determinations in the corresponding extracts also gave similar results. A small amount of lactate was formed after a long period of incubation. The activity of lactate dehydrogenase of *H. salinarium* is therefore increased when the growth medium is supplemented with glucose.

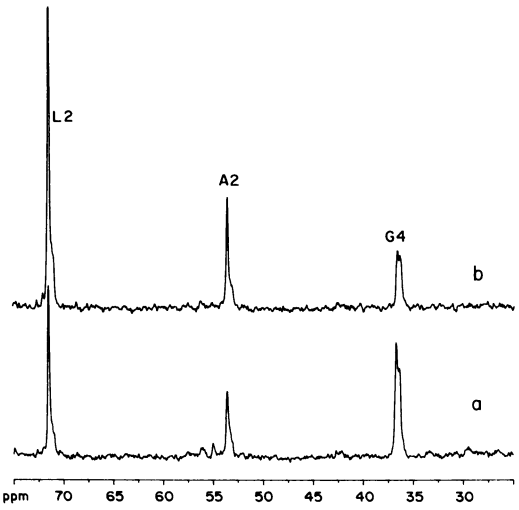

FIG. 2. Proton-decoupled ^{13}C NMR spectra of *H. salinarium* cells grown in the presence of glucose after incubation with [2-^{13}C]pyruvate with oxygen bubbling (a) and with nitrogen bubbling (b). Signal assignments are the same as in Fig. 1.

Production of C-2 alanine from [2-^{13}C]pyruvate is through transamination with endogenous, and therefore unlabelled, amino acids. The level of intensity of the signal is lower under aerobic conditions than under anaerobic conditions (Fig. 2). Again, this is expected, since more pyruvate is available for transamination in a situation in which the tricarboxylic acid cycle is less active. Supplementing the suspension medium with unlabelled aspartate increases the signal intensity. However, addition of glutamate did not significantly affect the [2-^{13}C]alanine signal. A transamination reaction with aspartate, but not with glutamate, thus seems to be the main source of labelled alanine. It is possible that glutamate is not being transported into the cells. Transport of glutamate into *H. salinarium* cells requires the presence of light and/or a Na^+ gradient (15). On the other hand glutamate:pyruvate transaminase may be absent in *H. salinarium*. This is evident from Fig. 2a in which the level of [2-^{13}C]alanine is low despite the high level of glutamate.

In cells grown in the absence of glucose (Fig. 3) or in the presence of acetate (Fig. 4), the signal intensity of [2-^{13}C]alanine is increased compared with that in glucose-grown cells (Fig. 2a). As mentioned earlier, under these conditions the

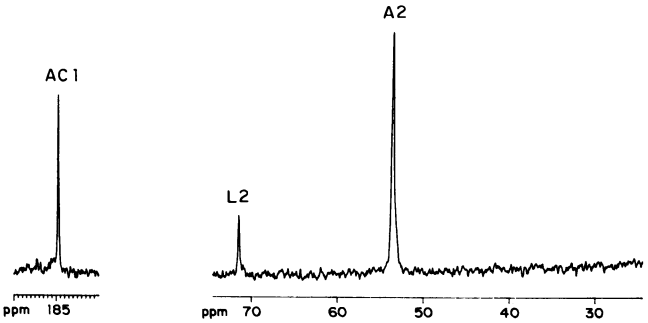

FIG. 3. Proton-decoupled ^{13}C NMR spectrum of *H. salinarium* cells grown in the absence of glucose after incubation with [2-^{13}C]pyruvate. AC1 is C-1 of acetate. Other resonances are as presented in Fig. 1.

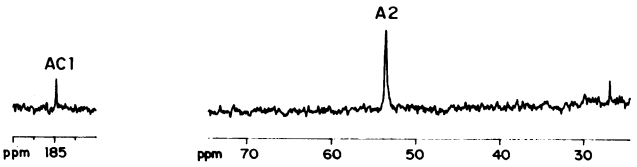

FIG. 4. Proton-decoupled ^{13}C NMR spectrum of *H. salinarium* cells grown in the presence of acetate after incubation with [2-^{13}C]pyruvate. Peak assignments are the same as in Fig. 3.

level of lactate dehydrogenase activity is lower. In addition, pyruvate entry into the tricarboxylic acid cycle is reduced, as is discussed later on. These two factors combine to make more labelled pyruvate available for formation of alanine.

Entry into the tricarboxylic acid cycle. Pyruvate enters into the tricarboxylic acid cycle as a two-carbon unit via acetyl-coenzyme A (CoA) through pyruvate:ferredoxin oxidoreductase. It might also be incorporated as oxaloacetate through the anaplerotic pyruvate carboxylase reaction. Figure 1 shows the ^{13}C NMR spectrum of glucose-grown *H. salinarium* cells incubated with [2-^{13}C]pyruvate. The resonances at 29.8, 36.4, and 184.5 ppm are assigned to C-3, C-4, and C-5 of glutamate, respectively. The formation of C-5-labelled glutamate (184.5 ppm) from [2-^{13}C]pyruvate is straightforward. The metabolic pathway followed is pyruvate → acetyl-CoA → citrate → isocitrate → α-ketoglutarate → glutamate. The flow of the label through this route is shown in Fig. 5. It can be inferred that the enzymes involved in these reactions are present in the cells. The presence of pyruvate:ferredoxin oxidoreductase and glutamate dehydrogenase in *H. salinarium* has been reported (5, 21). Isocitrate dehydrogenase, citrate synthase, and *cis*-aconitase have been observed in other halophilic bacteria also (1).

The formation of C-4-labelled glutamate (36.4 ppm) from

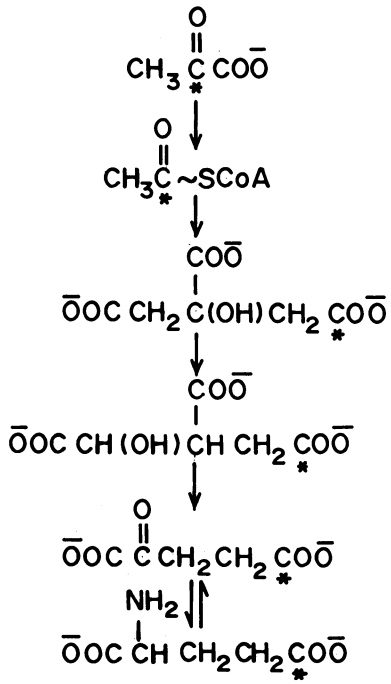

FIG. 5. Structure of intermediates and flow of label (asterisks) from [2-^{13}C]pyruvate to C-5 of glutamate.

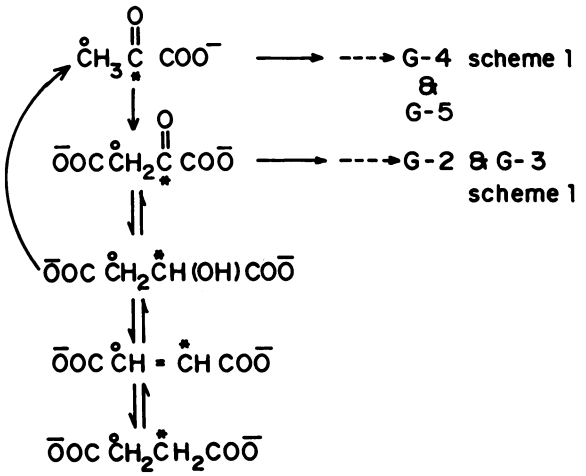

FIG. 6. Diagram showing structure of intermediates and flow of label (asterisks) from [2-^{13}C]pyruvate into C-2, C-3, C-4, and C-5 of glutamate. By carboxylation, pyruvate enters the tricarboxylic acid cycle through oxaloacetate. Scrambling of the label at the fumarate-succinate stage (o denotes label after scrambling) results in C-2- or C-3-labelled oxaloacetate. Furthermore, malic enzyme generates [3-^{13}C]pyruvate. These, in turn lead to C-2- or C-3- and C-4- or C-5-labelled glutamate. Scheme 1, Fig. 5.

[2-^{13}C]pyruvate is a little complicated. The pathway followed and the flow of the label are shown in Fig. 6. The pyruvate carboxylase reaction, label scrambling, and malic enzyme reaction seem to be the key factors in this route. Succinate dehydrogenase activity in *H. salinarium* has been reported (10). Malic enzyme activity in the cell extract was found in our experiments. By the pathway shown in Fig. 6, [3-^{13}C]pyruvate is formed, which follows the pathway shown in Fig. 5 to give C-4-labelled glutamate, but we do not see the resonance of C-3 alanine and C-3 lactate from [3-^{13}C]pyruvate. This may be because of the low concentration of [3-^{13}C]alanine and [3-^{13}C]lactate, which in turn is due to the malic enzyme being kinetically controlled to feed carbon skeletons effectively and unidirectionally into the tricarboxylic acid cycle (3).

The appearance of ^{13}C label at C-3 of glutamate can be explained by invoking the pyruvate carboxylase reaction. The pathway followed is C-2 pyruvate → C-2 oxaloacetate → C-3 citrate → C-3 isocitrate → C-3 α-ketoglutarate → C-3 glutamate. The scrambling of the oxaloacetate label between the 2 and 3 positions (the succinate-fumarate stage) would also result in some label at the C-2 of glutamate. However, the extent of labelling at this position is expected to be minuscule because of the diverging pathways at the malate and oxaloacetate stages (Fig. 7). As is evident from Fig. 1, C-2 glutamate is not observed.

The NMR spectra of cells grown in the absence of glucose and incubated with labelled pyruvate are shown in Fig. 3. Glutamate signals (29.8, 36.4, and 184.5 ppm) were not detected. Thus, pyruvate is not being used in the tricarboxylic acid cycle. However, a new signal was observed at 184.7 ppm. This was assigned to [1-^{13}C]acetate by comparison with an authentic sample. The levels of citrate synthase and malate synthase activities are known to be depressed in *H. salinarium* in media containing glucose (11). On the other hand, acetyl-CoA deacetylase activity is induced in this medium. Our observations suggest that in the presence of glucose, the condensing activity of citrate synthase is much greater than when the growth medium does not contain glucose. Also,

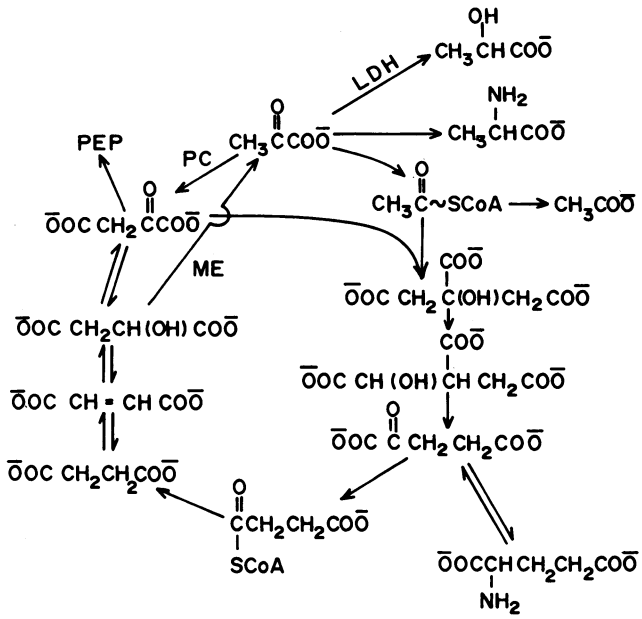

FIG. 7. Diagram showing various tricarboxylic acid cycle intermediates and other metabolic routes for utilization of pyruvate. Carbon units in pyruvate enter the tricarboxylic acid cycle either through acetyl-CoA to citrate or through carboxylation to oxaloacetate. LDH, lactate dehydrogenase; ME, malic enzyme; PC, pyruvate carboxylase; PEP, phosphoenolpyruvate.

acetyl-CoA deacetylase activity seems to be suppressed by glucose. An alternate explanation for the [1-^{13}C]acetate in cells grown in the absence of glucose is the increased residence time of acetyl-CoA (because of the reduced citrate synthase activity under this condition), which in turn leads to its enhanced hydrolysis. This has also been suggested earlier (11). However, [2-^{13}C]acetate is not detected. Malic enzyme activity is suppressed in the absence of glucose. Alternatively, in this case, oxaloacetate is selectively and quantitatively used for carbohydrate synthesis through phosphoenolpyruvate carboxykinase and reversed glycolysis (6, 22), and so the flux of oxaloacetate through malate → fumarate → succinate → fumarate → malate → pyruvate, and thence to [2-^{13}C]acetate, is reduced. Cells grown in the presence of acetate showed similar results.

Operation of the whole tricarboxylic acid cycle will also give resonance for C-1-labelled glutamate and labelled CO_2 from the second turn onwards. However, neither of these signals was observed in our experiments, even after prolonged incubation with [2-^{13}C]pyruvate. This result indicates that, although production of glutamate through the tricarboxylic acid cycle is occurring, the labelling of the intermediates of the cycle does not proceed beyond α-ketoglutarate. However, the presence of an α-ketoglutarate dehydrogenase and succinyl-CoA synthetase in *H. salinarium* has been reported (1, 13). Thus, it seems likely that the α-ketoglutarate dehydrogenase reaction is blocked, since it is known that parapyruvate—an adduct of pyruvate—competitively inhibits this reaction (14). Furthermore, in our experiments, we found that the NMR spectra of cells with malonate in the incubation medium were similar to those of cells in media without malonate. In addition, ^{13}C-^{13}C couplings were not observed, suggesting that adjacent carbon positions were not enriched and that only monolabelled glutamate (C-3, C-4, and C-5) is formed. This is as expected if [2-^{13}C]pyruvate is the substrate. This has also been reported by Evans et al. (8). The observation of similar patterns of labelling of glutamate in the presence or absence of malonate is surprising. With *E. coli*, Evans et al. (8) observed no enrichment of glutamate from labelled propionate when malonate was included in the incubation medium. They suggested the presence of a highly organized tricarboxylic acid cycle multienzyme cluster which results in tight substrate channeling. This blocks the entry of propionate into the cycle through propionyl-CoA and acetyl-CoA pathways if one of the enzymes in the cluster is inhibited (8). Our results with *H. salinarium* indicate that tricarboxylic acid cycle enzymes diffuse freely and thus lead to accumulation of glutamate labelled at C-3, C-4, and C-5, depending on whether the entry point is acetyl-CoA or oxaloacetate.

ACKNOWLEDGMENTS

We gratefully acknowledge help from the FT-NMR National Facility funded by the Department of Science and Technology and located at the Tata Institute of Fundamental Research, Bombay, where the NMR experiments were performed.

REFERENCES

1. **Aitken, D. M., and A. D. Brown.** 1969. Citrate and glyoxylate cycles in the halophile *Halobacterium salinarium*. Biochim. Biophys. Acta **177**:351–354.
2. **Badar-Goffer, R., and H. Bachalard.** 1991. Metabolic studies using ^{13}C nuclear magnetic resonance spectroscopy. Essays Biochem. **26**:105–119.
3. **Bailey, I. A., D. G. Gadian, P. M. Mathews, G. K. Radda, and P. J. Seeley.** 1981. Studies of metabolism in the isolated, perfused rat heart using ^{13}C NMR. FEBS Lett. **123**:315–318.
4. **Ben-Yoseph, O., R. Badar-Goffer, P. G. Morris, and H. Bachalard.** 1993. Glycerol-3-phosphate and lactate as indicators of the cerebral cytoplasmic redox state in severe and mild hypoxia, respectively: a ^{13}C and ^{31}P NMR study. Biochem. J. **291**:915–919.
5. **Bonete, M. J., M. L. Camacho, and E. Cadenas.** 1986. Purification and some properties of NAD$^+$-dependent glutamate dehydrogenase from *Halobacterium halobium*. Int. J. Biochem. **18**:785–789.
6. **D'Souza, S. E., and W. Altekar.** 1983. Demonstration of some glycolytic activities in *Halobacterium halobium* and their significance. Indian J. Biochem. Biophys. **20**:29–32.
7. **Elazari-Volcani, B.** 1957. Genus XII. *Halobacterium*, p. 207–212. *In* R. S. Breed, E. G. D. Murray, and N. R. Smith (ed.), Bergey's manual of determinative bacteriology, 7th ed. Williams and Wilkins, Baltimore.
8. **Evans, C. T., B. Sumegi, P. A. Srere, A. D. Sherry, and C. R. Malloy.** 1993. [^{13}C]propionate oxidation in wild-type and citrate synthase mutant *Escherichia coli*: evidence for multiple pathways of propionate utilization. Biochem. J. **291**:927–932.
9. **Frydman, B., C. D. L. Santos, J. B. Cannata, and J. J. Cazzulo.** 1990. Carbon-13 nuclear magnetic resonance analysis of [1-^{13}C]glucose metabolism of *Trypanosoma cruzi*. Evidence of the presence of two alanine pools and of two CO_2 fixation reactions. Eur. J. Biochem. **192**:363–368.
10. **Gradin, C. H., L. Hederstedt, and H. Baltscheffsky.** 1985. Soluble succinate dehydrogenase from halophilic archaebacterium, *Halobacterium halobium*. Arch. Biochem. Biophys. **239**:200–205.
11. **Hochstein, L. I.** 1978. Carbohydrate metabolism in the extremely halophilic bacteria: the role of glucose in the regulation of citrate synthase activity, p. 397–412. *In* S. R. Caplan and M. Ginzburg (ed.), Energetics and structure of halophilic microorganisms. Elsevier/North-Holland Biomedical Press, Amsterdam.
12. **Jans, A. W. H., and R. Willem.** 1989. A ^{13}C NMR investigation of the metabolism of amino acids in renal proximal convoluted tubules of normal and streptozotocin-treated rats. Biochem. J. **263**:231–241.
13. **Kerscher, L., and D. Oesterhelt.** 1981. Purification and properties of two 2-oxoacid:ferredoxin oxidoreductases from *Halobacterium halobium*. Eur. J. Biochem. **116**:587–594.
14. **Korff, R. W. V.** 1969. Purity and stability of pyruvate and α-ketoglutarate. Methods Enzymol. **13**:519–523.

15. **Lanyi, J. K.** 1978. Transport of cations and amino acids in *Halobacterium halobium*, p. 415–423. *In* S. R. Caplan and M. Ginzburg (ed.), Energetics and structure of halophilic microorganisms. Elsevier/North-Holland Biomedical Press, Amsterdam.
16. **Larsen, H.** 1962. Halophilism, p. 297. *In* I. C. Gunsalus and R. Y. Stanier (ed.), The bacteria, a treatise on structure and function. Academic Press, New York.
17. **Lowry, O. H., N. J. Rosebrough, A. L. Farr, and R. J. Randall.** 1951. Protein measurement with the Folin phenol reagent. J. Biol. Chem. **193:**265–275.
18. **Malloy, C. R., A. D. Sherry, and F. M. H. Jeffrey.** 1990. Analysis of tricarboxylic acid cycle of the heart using ^{13}C isotope isomers. Am. J. Physiol. **259:**H987–H995.
19. **Matwiyoff, N. A., R. E. London, and J. Y. Hutson.** 1982. The study of the metabolism of ^{13}C labeled substrates by ^{13}C NMR spectroscopy of intact cells, tissues, and organs, p. 157–186. *In* G. C. Levy (ed.), NMR spectroscopy: new methods and applications. American Chemical Society, Washington, D.C.
20. **Narbad, A., M. J. E. Hewlino, P. Gacasa, and N. J. Russel.** 1990. The use of ^{13}C NMR spectroscopy to monitor alginate biosynthesis in mucoid *Pseudomonas aeruginosa*. Biochem. J. **267:**579–584.
21. **Plaga, W., F. Lottspeich, and D. Oesterhelt.** 1992. Improved purification and primary structure of pyruvate:ferredoxin oxidoreductase from *Halobacterium halobium*. Eur. J. Biochem. **205:**391–397.
22. **Rawal, N., S. M. Kelkar, and W. Altekar.** 1988. Alternative routes of carbohydrate metabolism in halophilic Archaebacteria. Indian J. Biochem. Biophys. **25:**674–686.
23. **Sonawat, H. M., S. Srivastava, S. Swaminathan, and G. Govil.** 1990. Glycolysis and Entner-Doudoroff pathways in *Halobacterium halobium*: some new observations based on ^{13}C NMR spectroscopy. Biochem. Biophys. Res. Commun. **173:**358–362.